Signature of deconfinement with spin down compression in cooling hybrid stars

Morten Stejner
Department of Physics and Astronomy, University of Aarhus
Ny Munkegade, Bld. 1520, DK-8000 Aarhus C, Denmark.
msp@phys.au.dk
and

Fridolin Weber
Department of Physics, San Diego State University
5500 Campanile Dr, San Diego CA 92182-1233
and

Jes Madsen
Department of Physics and Astronomy, University of Aarhus
Ny Munkegade, Bld. 1520, DK-8000 Aarhus C, Denmark.

ABSTRACT

The thermal evolution of neutron stars is coupled to their spin down and the resulting changes in structure and chemical composition. This coupling correlates stellar surface temperatures with rotational state as well as time. We report an extensive investigation of the coupling between spin down and cooling for hybrid stars which undergo a phase transition to deconfined quark matter at the high densities present in stars at low rotation frequencies. The thermal balance of neutron stars is re-analyzed to incorporate phase transitions and the related latent heat self-consistently, and numerical calculations are undertaken to simultaneously evolve the stellar structure and temperature distribution. We find that the changes in stellar structure and chemical composition with the introduction of a pure quark matter phase in the core delay the cooling and produce a period of increasing surface temperature for strongly superfluid stars of strong and intermediate magnetic field strength. The latent heat of deconfinement is found to reinforce this signature if quark matter is superfluid and it can dominate the thermal balance during the formation of a pure quark matter core. At other times it is less important and does not significantly change the thermal evolution.

Subject headings: Stars:neutron — stars:rotation — dense matter — equation of state

1. Introduction

The chemical composition of neutron stars at densities beyond nuclear saturation remains uncertain with alternatives ranging from purely nucleonic compositions through hyperon or meson condensates to deconfined quark matter – see e.g. Weber (2005) and Page & Reddy (2006) for recent reviews with emphasis on quark matter. A future understanding of neutron star structure gained through confrontation of theoretical models with the now steadily growing body of observational facts will therefore simultaneously constrain fundamental elements of particle and nuclear physics (Lattimer & Prakash 2007). The interlinked processes of spin down and thermal cooling present intriguing prospects of gaining insight in the properties of matter in neutron star cores by confrontation with soft X-ray observations of thermal radiation from neutron star surfaces as they both depend sensitively on and to some extent determine the chemical composition.

As neutron stars spin down and contract, their structure and composition change with the increasing density – drastically if phase boundaries are crossed so new forms of matter become possible. We shall here investigate how this influences the thermal evolution of hybrid stars which contain large amounts of deconfined quark matter. The increasing density and changing chemical composition further imply additional entropy production in bulk and the release of latent heat as particles cross any phase boundaries present. We therefore re-analyze the thermal equilibrium of compact stars to show how mixed phases may be incorporated. We thus arrive at a natural description of the latent heat of phase transitions in compact stars, but also find – through direct numerical calculations – that unless the stellar structure changes very rapidly the effects of latent heat on the thermal evolution are insignificant when compared to those of the changing chemical composition and the surface area reduction.

Neutron stars are extremely compact objects and densities in their cores reach well in excess of the nuclear saturation density. At such densities the distance between particles is on the order of the characteristic range of the nuclear forces. Therefore, as was stressed recently by Baym (2007), perturbative treatments in terms of few- or even many-body forces – although highly successful in describing the properties of matter below nuclear saturation – are no longer well defined in the core of neutron stars. Further, the relevant degrees of freedom should include the appearance of hyperons and possibly deconfined quarks, so treatments in terms of nucleons alone must also be seen as approximative. Hyperons are expected to appear at densities around $2-3\rho_0$, where $\rho_0 = 0.153$ fm^{-3} is the baryon density at nuclear saturation. The appearance of hyperons so softens the equation of state that purely hadronic equations of state may not allow stable models compatible with the accurately measured masses of neutron stars in binary systems (Baldo et al. 2003; Schulze et al. 2006). Schulze et al. (2006) further demonstrate that this conclusion is highly robust with respect to different assumptions about hyperon interactions and the nucleonic equation of state. At best these studies are strong arguments against purely hadronic compositions and they certainly do show the relevance of considering alternatives such as a transition at high densities to deconfined quark matter.

Quark matter represents an entirely new type of matter – as opposed to just an additional degree of freedom as in the case of hyperons in the hadronic phase – and it cannot be assumed to soften the equation of state to the same extent (Alford et al. 2008;

Schaffner-Bielich 2007). Hybrid stars can be be consistent with the high masses and radii indicated by recent observations (e.g. Özel (2006), Freire et al. (2008b,a); Freire (2008)), and the quark matter equation of state can fulfill the constraints imposed by heavy-ion collision transverse flow data and K^+ production (which nucleonic equations of state do not). Further, Drago et al. (2008) found that only stars with a quark matter component can rotate stably without losing angular momentum by emission of gravitational waves through the r-mode instability at the 1122 Hz indicated by recent observations for the X-ray transient XTE J1739-285 (Kaaret et al. 2007). This conclusion is tentative as the observed neutron star spin frequency awaits confirmation, but it again shows how the composition of neutron stars is an open question to be determined by a confrontation of theory and observation, and that a deconfined quark matter phase remains a viable alternative.

For definiteness we shall work with the equation of state suggested by Glendenning (1992); hereafter the G_{180}^{300} equation of state. While this equation of state is not sophisticated in its treatment of the quark matter phase, it is illustrative in that it allows a very large pure quark matter core with a transition through a mixed phase at relatively low densities around 2-5ρ_0. For our purposes it is interesting in that it implies drastic changes in composition with spin down – the pure quark matter core disappears at high spin frequencies for instance – and it therefore represents something close to a limiting case. We shall then be able to investigate both the effects of steady conversion of hadronic matter to quark matter and the sudden appearance of a pure quark matter core in the hadronic phase.

In the so-called minimal scenario, which excludes exotic and very rapid neutrino processes (Page et al. 2004), the internal temperature of neutron stars drops from beyond 10^{10} K to around 10^9 K within a few minutes after their birth, and neutrino cooling continues to dominate for at least the next few thousand years until the internal temperature has dropped below 10^8 K and photon cooling takes over (see, e.g. Page et al. (2004); Yakovlev & Pethick (2004) for reviews). If the highly efficient direct Urca neutrino emission (i.e., essentially beta decays, $n \rightarrow p + e^- + \bar{\nu}_e$ and related processes in quark matter) is active, the stars may cool very rapidly and reach very low temperatures on a timescale of a few hundred years. As we shall see the nuclear direct Urca process is active in the mixed phase of hybrid stars, and may thus control the thermal evolution. These processes may be suppressed by pairing of the participating particles however, and further the extent of the mixed phase depends strongly on the rotation frequency thus giving rise to a diverse range of possible cooling paths.

The latent heat of the phase transition and the related release of entropy in bulk with changing density are generally found to be of smaller importance than the changing structure and chemical composition. It does not significantly delay or enhance the cooling, although it does briefly balance or even dominate the cooling terms when the pure quark matter core is first formed for certain choices of stellar parameters. The latent heat of the quark matter phase transition was previously considered by Miao & Xiao-Ping (2007); Miao et al. (2007) and, Xiaoping et al. (2008). These authors took a different approach to calculate the latent heat than what is discussed below and found very significant heating terms which we do not recover.

The work of Reisenegger (1995) and lately Fernández & Reisenegger (2005) considered the related process of roto-chemical heating for neutron stars in which weak reactions are driven out of equilibrium by the changing den-

sity. The resulting release of energy was found able to maintain old stars at relatively high temperatures determined by their rate of spin down. This term naturally appears in our equations for the thermal balance and should be included in a full model. It is to some extent complementary to the effects discussed here, but the treatment of weak reactions beyond equilibrium is beyond our scope in this work, and we shall assume chemical equilibrium throughout. We return briefly to discuss this issue in Sect. 5.

The link between the thermal evolution of neutron stars and their spin down has become a subject of some interest as an observational correlation between the temperatures and inferred magnetic fields of neutron stars was recently discovered by Pons et al. (2007). This was interpreted as evidence for magnetic field decay and detailed work by Aguilera et al. (2008,?) strongly supports this conclusion. An alternative interpretation was offered recently by Niebergal et al. (2007) in terms of magnetic flux expulsion from color-flavor locked quark stars (a hypothetical class of stars consisting entirely of quark matter which in this case is assumed to be absolutely stable). The previously mentioned work of Drago et al. (2008) also indicates a link between the spin down and cooling of hybrid stars. These correlations – if they can indeed be shown to exist – complement the traditional cooling calculations which relate only temperature and age, and they may help break the degeneracy seen between such calculations with different underlying assumptions about the state of matter at very high density.

In the following, we shall first revisit the equations of thermal balance for compact stars in Sect. 2 to show the effects of a time-dependent density and discuss how the presence of phase transitions may be included. In Sect. 3, we discuss the G_{180}^{300} equation of state, the resulting stellar models and some simple estimates for the additional terms in the thermal balance equations in more detail. In Sect. 4 we show the results of including these terms in spherical isothermal cooling calculations. We conclude with a discussion in Sect. 5.

2. Thermal Equilibrium in the Mixed Phase

The thermal evolution of compact stars is determined by the equations of local energy conservation and transport in the framework of general relativity. These equations balance any energy radiated away from the star by photons and neutrinos against changes in rest mass due to nuclear reactions and changes in gravitational or internal energy as the stellar structure evolves. In the most widely studied scenario the stellar structure is assumed constant and the only energy source available to neutron stars is then their original endowment of thermal energy (e.g., Van Riper (1991); Schaab et al. (1996); Page et al. (2004, 2006); Yakovlev & Pethick (2004) and references therein). Neutrino production in the core and photon emission from the stellar surface then ensures a monotonical and sometimes very rapid cooling of the star depending strongly on any superfluid properties of the core. But in addition to this a number of powerful energy sources may play a role in delaying or even reversing the cooling at various stages in a neutron stars life – see e.g. Schaab et al. (1999) for an overview of possible sources and their effects. Here we discuss the effects of including a phase transition in the energy balance, which, as the stellar structure changes, must then also include redistribution of entropy between the two phases as their proportion changes as well as changes in surface and Coulomb energy for transitions through a mixed phase.

Following Thorne (1966) or the equivalent discussion in Weber (1999) we consider energy conservation for a spherical shell inside of which is a baryons and which itself contains δa baryons. The treatment given in this section therefore assumes spherical symmetry which is sufficient to show the effects of a phase transition on local energy conservation – we shall return later to discuss possible consequences of a multidimensional cooling calculation. The shell under consideration will change its internal energy during a coordinate time interval dt by

$$\begin{aligned} & d(\text{internal energy}) = \\ & (\text{amount of rest mass-energy converted to} \\ & \text{internal energy by reactions}) \\ + \quad & (\text{work done on shell by gravitational} \\ & \text{forces to change its volume during} \\ & \text{quasi-static contraction}) \\ - \quad & (\text{energy radiated, conducted} \\ & \text{or convected away from the shell}). \end{aligned} \tag{1}$$

It is important to note at this point that if the two phases are in equilibrium – as should certainly be expected for transitions governed by strong reactions such as that from hadronic to quark matter – there is *no binding energy* involved in the transition and therefore no contribution to the first term on the right hand side of Eq. (1). If this was the case and the phase transition did involve a binding energy the two phases could not be in equilibrium and the star would adjust itself accordingly – eventually becoming a strange star in the case of the quark matter transition if quark matter was assumed bound relative to hadronic matter at zero external pressure. In hybrid stars this is not the assumption however, and so any latent heat evolved or absorbed in the phase transition follows from the different thermodynamical properties of the two phases as with any other phase transition.

In the mixed phase of the G_{180}^{300} equation of state regions containing negatively charged quark matter appear at densities of about 2 times nuclear saturation and dominate completely at 5 times nuclear saturation. They allow the hadronic matter to lower its isospin asymmetry energy and become positively charged by including more protons with charge neutrality achieved globally. The geometry and structure of the mixed phase is determined by a balance between surface tension and Coulomb repulsion between regions of like charge. For details on the phase transition we refer to e.g. Glendenning (1992); Heiselberg et al. (1993); Glendenning (2000); Glendenning & Weber (2001); Voskresensky et al. (2003); Endo et al. (2006).

Returning to our spherical shell of baryon number δa we will assume that its volume V is large enough to contain a macroscopic number of unit cells each containing a region filled by the rare phase whose presence may then be considered a microscopic property of the equation of state. The work done to change the shells volume during contraction or expansion of the star must then include changes in surface and Coulomb energy as well as the usual pressure term

$$\mathrm{d}W = -P\mathrm{d}V + \alpha \mathrm{d}\mathbb{S} + \mathrm{d}E_{\mathrm{C}} \tag{2}$$

where α is the surface tension, $\mathbb{S}$ is the amount of surface area in the shell dividing the two phases and E_{C} is the Coulomb energy contained in the shell. These terms can be similarly included in the first law of thermodynamics which we write in the same notation (units with $G = c = k_{\mathrm{B}} = 1$ will be used here and throughout this paper)

$$\begin{aligned} \mathrm{d}\epsilon = \; & \tfrac{P+\epsilon}{\rho}\mathrm{d}\rho + T\rho \mathrm{d}s + \textstyle\sum_k \mu_k \rho \mathrm{d}Y_k \\ & + \rho \tfrac{\alpha \mathrm{d}\mathbb{S}}{\delta a} + \rho \tfrac{\mathrm{d}E_{\mathrm{C}}}{\delta a} \end{aligned} \tag{3}$$

where s is the entropy per baryon and $Y_{\mathrm{k}} = \rho_k/\rho$ is the fraction of the baryon number den-

sity in the form k with k running over all particle species and $\sum_k Y_k = 1$. In the quark matter phase each quark contributes by only $\frac{1}{3}$ to the baryon number density and s is then the entropy per three quarks. The last two terms in Eq. (3) are the local densities of surface and Coulomb energy written in a form useful for our purpose.

Inserting this in Eq. (1) and using that the amount of energy radiated, conducted or convected away from the shell can be written in terms of the gradient of the total luminosity, $L_{\rm tot}$, we show in Appendix A that local energy balance may be expressed as

$$\frac{\mathrm{d}}{\mathrm{d}a}(L_{\rm tot}e^{2\Phi}) = -e^{\Phi}\left[T\left(\frac{\mathrm{d}s}{\mathrm{d}t}\right)_a + \sum_k \mu_k \left(\frac{\mathrm{d}Y_k}{\mathrm{d}t}\right)_a\right] \tag{4}$$

thus giving the contribution to $L_{\rm tot}$ from the shell in terms of the entropy production and the difference between the chemical potentials of particles participating in any reactions taking place in the shell. $e^{2\Phi}$ is the time component of a spherically symmetric metric

$$ds^2 = -e^{2\Phi}dt^2 + e^{2\Lambda}dr^2 + r^2 d\theta^2 + r^2\sin\theta^2 d\Phi^2 \tag{5}$$

found from the general relativistic structure equations for compact stars.

$L_{\rm tot}$ includes the neutrino luminosity, but since neutrinos can be taken to immediately escape from the star when they are created without converting into any other form of energy along the way, they fulfill their own separate equation of energy conservation

$$\frac{\mathrm{d}}{\mathrm{d}a}(L_\nu e^{2\Phi}) = \frac{\epsilon_\nu}{\rho}e^{2\Phi} \tag{6}$$

where L_ν is the neutrino luminosity and ϵ_ν is the neutrino emissivity; the rate per unit volume at which neutrino energy is created. In neutron stars convection is negligible compared to electron conduction and photon diffusion and so the remainder of $L_{\rm tot}$ can be shown to fulfill a transport equation (Thorne 1966; Weber 1999)

$$\frac{\mathrm{d}}{\mathrm{d}a}\left(Te^{\Phi}\right) = -\frac{3}{16\sigma}\frac{\kappa\epsilon}{T^3}\frac{Le^{\Phi}}{16\pi^2 r^4\rho} \tag{7}$$

where σ is the Stefan-Boltzmann constant, κ is the total thermal conductivity and $L = L_{\rm tot} - L_\nu$. At the stellar center we must have $L_{\rm tot}(a=0) = 0$ while at the stellar surface L must equal the total stellar photon luminosity which may depend on assumptions about properties of the stellar atmosphere or lack thereof.

Eqs. (4)-(7) with the appropriate boundary conditions can be solved to evolve the thermal structure of a stellar model. They have exactly the same form as would be expected in the absence of any phase transitions. However, the phase transition influences the entropy density and this, as we shall see, gives rise to additional terms in the heat balance including latent heat and the surface and Coulomb energies. An equivalent form of Eq. (4) showing the contributions from surface and Coulomb terms more explicitly can be found in Eq. (A6) of Appendix A. Combining Eqs. (4) and (6), noting that $c_{\rm v} = \rho T(\partial s/\partial T)_V$ and assuming constant structure and chemical composition we also recover the standard cooling equation for static stars

$$\frac{\mathrm{d}}{\mathrm{d}a}(Le^{2\Phi}) = -\rho^{-1}\left(\epsilon_\nu e^{2\Phi} + c_{\rm v}\frac{\mathrm{d}(Te^{\Phi})}{\mathrm{d}t}\right) \tag{8}$$

Eq. (4) is useful because it allows a particularly simple analysis in the presence of a phase transition. The first thing to note is, that particles crossing the phase boundary would not contribute to the second term on the right hand side of Eq. (4) if the two phases are in or close to equilibrium, because their chemical potentials (or those of their constituents) must then be continuous across the phase

boundary. In the following we therefore neglect this term, but we shall return to discuss its potential importance for reactions not in equilibrium. The first term is a different matter however. The entropy per particle is a function of density, temperature and chemical composition which is not required to be continuous across the phase boundary, so particles making the transition will release or absorb heat accordingly. To see how this works we write s as a sum with bulk contributions from each phase according to their volume or mass fraction as well as contributions from the surface and Coulomb energies

$$s = \frac{1}{\rho}((1-\chi_{\rm v})S_1 + \chi_{\rm v}S_2 + S_{\rm S} + S_{\rm C}) \quad (9)$$

$$= (1-\chi_\rho)s_1 + \chi_\rho s_2 + \frac{1}{\rho}(S_{\rm S} + S_{\rm C}) \quad (10)$$

where $\rho = (1-\chi_{\rm v})\rho_1 + \chi_{\rm v}\rho_2$ is the average of the two particle densities $\rho_{1,2}$ weighed by the volume fraction of the dense phase, $\chi_{\rm v}$. $S_{1,2}$ is the bulk entropy density in each phase and $S_{\rm S}$ and $S_{\rm C}$ are the surface and Coulomb contributions to the entropy density respectively. We have further introduced the baryon number fraction χ_ρ of baryons in the dense phase in a sample of matter related to the volume fraction by $\chi_\rho = \chi_{\rm v}(\rho_2/\rho)$, as well as the entropies per baryon in the respective phases, $s_{1,2} = S_{1,2}/\rho_{1,2}$. At constant a and assuming the fraction of matter in the dense phase and the particle densities do not depend on temperature we then have

$$\begin{aligned} T\frac{{\rm d}s}{{\rm d}t} &= \frac{c_{\rm v}}{\rho}\frac{{\rm d}T}{{\rm d}t} + T\frac{{\rm d}s}{{\rm d}\rho}\frac{{\rm d}\rho}{{\rm d}t} \\ &= \frac{c_{\rm v}}{\rho}\frac{{\rm d}T}{{\rm d}t} + T\frac{{\rm d}\chi_\rho}{{\rm d}\rho}\frac{{\rm d}\rho}{{\rm d}t}(s_2 - s_1) \\ &\quad +(1-\chi_\rho)T\frac{{\rm d}\rho}{{\rm d}t}\frac{{\rm d}s_1}{{\rm d}\rho} + \chi_\rho T\frac{{\rm d}\rho}{{\rm d}t}\frac{{\rm d}s_2}{{\rm d}\rho} \\ &\quad +T\frac{\rm d}{{\rm d}t}\left[\frac{1}{\rho}(S_{\rm S} + S_{\rm C})\right] \end{aligned} \quad (11)$$

where the heat capacity is again a weighed volume average in the mixed phase

$$c_{\rm v} = (1-\chi_{\rm v})c_{{\rm V},1} + \chi_{\rm v}c_{{\rm V},2}\,. \quad (12)$$

The latent heat absorbed by a particle crossing the boundary between two phases in equilibrium is the temperature times the difference in entropy per particle between the two phases, $q = T[s_2 - s_1]$ (Landau & Lifshitz 1980); we recover this in the second term on the right hand side of Eq. (11). If any term in Eq. (11) is negative, heat is evolved by this term which then heats the star and adds to the luminosity L. In particular the latent heat is a heating term for increasing density when the entropy per baryon of the dense phase is less than that of the low density phase – a situation which will arise when considering superfluid quark matter.

For future reference we identify the terms in Eq. (11) as follows. $T\frac{{\rm d}\chi_\rho}{{\rm d}\rho}\frac{{\rm d}\rho}{{\rm d}t}(s_2 - s_1)$ is identified as the latent heat, $(1-\chi_\rho)T\frac{{\rm d}\rho}{{\rm d}t}\frac{{\rm d}s_1}{{\rm d}\rho}$ is identified as the hadronic bulk contribution, $\chi_\rho T\frac{{\rm d}\rho}{{\rm d}t}\frac{{\rm d}s_2}{{\rm d}\rho}$ is identified as the quark bulk contribution, and the last term $T({\rm d}/{\rm d}t)[(S_{\rm S} + S_{\rm C})/\rho]$ is identified as the surface and Coulomb contribution. Further we often refer to these terms collectively as additional entropy production (or release) beyond what would be expected at constant density.

We discuss in the following section how to calculate the bulk entropy density of the hadronic and quark matter phases in the relativistic mean field theory framework of the $\rm G_{180}^{300}$ equation of state. For now let us just remark that the entropy per particle for an ideal relativistic degenerate Fermi gas is (Landau & Lifshitz 1980)

$$s = \frac{(3\pi^2)^{\frac{2}{3}}}{3\hbar c}T\rho^{-\frac{1}{3}} = 0.02\frac{T}{\rm MeV}\left(\frac{\rho}{\rm fm^{-3}}\right)^{-\frac{1}{3}}\,. \quad (13)$$

Taking the transition to quark matter as a transition between such gases – note that the

bag constant does not contribute to the entropy – and remembering that each hadron contains three quarks which further have a color degeneracy of three, the latent heat in Eq. (11) is of the order of

$$10^{33}T_9^2\left[9\left(\frac{\rho_{\rm Q}}{\rm fm^{-3}}\right)^{-\frac{1}{3}}-\left(\frac{\rho_{\rm H}}{\rm fm^{-3}}\right)^{-\frac{1}{3}}\right] \times \frac{{\rm d}a_{\rm Q}/{\rm d}t}{10^{57}/10^7\ {\rm yr}}\ {\rm erg\ s^{-1}} \quad (14)$$

where $T_9 = T/10^9$ K, and the rate of baryons making the transition to quark matter, ${\rm d}a_{\rm Q}/{\rm d}t$, was (arbitrarily) scaled to an entire star being converted steadily over 10^7 years. Unless the star is very hot or changing structure fast this is a very modest contribution, and we further note that it is positive for a contracting star and so acts to cool the star down. However the sign is subject to the very rough assumption that both gases may be treated as ideal Fermi gases for the purpose of calculating their entropy, and it will change in a more detailed treatment. Specifically the quark phase may be color-superconducting with energy gaps as high as 100 MeV and corresponding critical temperatures of the order of 10^{11} K. Below the critical temperature the quark specific heat and entropy density would be exponentially suppressed and could be ignored relative to the hadronic contribution in Eq. (14) which would then be a heating term. We shall return to both possibilities in later sections.

We shall calculate the two bulk terms numerically in the following sections, so for now we just note that from Eq. (13) the entropy per baryon decreases with increasing density. In a contracting star these terms will hence act as heating terms and locally be of the same order of magnitude as the release or absorption of latent heat in Eq. (14) – but of course they contribute throughout the star and are therefore potentially far more important than the latent heat which is only significant in the mixed phase.

Since the surface and Coulomb energies are related by $E_{\rm S} = 2E_{\rm C}$ in equilibrium (Glendenning 2000), their contributions to the thermodynamic potential, and hence to the entropy, are similarly fixed in proportion, and we need only consider one of them here. Specifically the surface part of the entropy may be found from (Landau & Lifshitz 1980)

$$\Omega = \Omega_0 + \Omega_{\rm S} = \Omega_0 + \alpha\mathbb{S} \quad (15)$$

$$S_{\rm S} = -\frac{\partial\Omega_{\rm S}}{\partial T} = -\mathbb{S}\frac{\partial\alpha}{\partial T}\ , \quad (16)$$

where $\Omega_{\rm S}$ is the surface contribution to the thermodynamic potential Ω. The surface tension for the quark-hadron interface, α, determines the geometry and extent of the mixed phase (Glendenning 1992; Heiselberg et al. 1993; Voskresensky et al. 2003; Endo et al. 2006). The surface tension of strangelets in vacuum has been evaluated by Berger & Jaffe (1987), but the surface tension for the mixed phase remains essentially unknown. It is commonly parameterized as being proportional to the difference in energy density between the two phases and the length scale $L \sim 1$ fm of the strong interaction (Glendenning 2000)

$$\alpha = K \times [\epsilon_{\rm Q} - \epsilon_{\rm H}] \times L\ . \quad (17)$$

Assuming for simplicity that K and L are constant we then get

$$\frac{\partial\alpha}{\partial T} = \alpha\frac{c_{\rm V,Q} - c_{\rm V,H}}{\epsilon_{\rm Q} - \epsilon_{\rm H}} \quad (18)$$

$$\rho^{-1}(S_{\rm S} + S_{\rm C}) = -\frac{3}{2}\frac{\epsilon_{\rm S}}{\rho}\frac{c_{\rm V,Q} - c_{\rm V,H}}{\epsilon_{\rm Q} - \epsilon_{\rm H}} \quad (19)$$

The corresponding term in Eq. (11) is then of the order of the surface energy per baryon times the ratio between thermal and total energy density. It can therefore not be expected to contribute significantly, and this expectation is confirmed by the numerical results.

3. Equation of State and Stellar Models

In our numerical work we have employed the rotating neutron star code developed by Weber and the G_{180}^{300} equation of state used by Glendenning (1992, 2000) and Glendenning & Weber (2001). Here we shall briefly describe each of these and the resulting stellar models.

The G_{180}^{300} equation of state treats the deconfined quark matter phase in a simple version of the bag model which ignores gluon interactions. The confined hadronic phase is described in terms of the mean field solution to a covariant Lagrangian that involves the baryon octet interacting through scalar, vector and vector-isovector mesons. The precise values of the coupling constants for the hadronic part of the model correspond to the first set of Table 5.5 of Glendenning (2000) or Table 1 of Glendenning & Weber (2001). For details we refer to these works where the resulting equation of state as well as the underlying theory are carefully described at zero temperature. Finite temperature expressions for pressure, energy and particle densities can be found by reinserting the Fermi distribution in the phase space integrals of their zero temperature expressions which we shall not write explicitly here. We refer to e.g. Glendenning (1990) for the full temperature dependent expressions (this reference also includes gluon interactions to first order which we ignore here).

The entropy is calculated as

$$s = \frac{1}{\rho T}\left[P + \epsilon - \sum_i \mu_i \rho_i\right] \qquad (20)$$

using the finite temperature expressions outlined above and using the highly accurate publicly available code described in Miralles & van Riper (1996) to solve the Fermi integrals. In keeping with our assumption that temperatures remain too low to significantly influence the chemical composition we neglect contributions from thermally exited particle-antiparticle pairs.

Figs. 1 and 2 show the resulting chemical composition and entropy. In the quark phase we note that u-quarks are suppressed initially giving the phase a negative net charge, and that as expected the entropy per baryon – though not per quark – is higher in the quark matter phase in the absence of any pairing phenomena. We have checked numerically that in the absence of pairing the entropy simply scales linearly with temperature within the temperature range we shall need.

The sum of the surface and Coulomb energies has a maximum as a function of density around $\rho = 0.5 - 0.6$ fm^{-3} with a corresponding minimum in the related entropy in Fig. 3. The surface and Coulomb term in Eq. (11) can therefore be either positive or negative and either heat or cool the star accordingly. The surface and Coulomb contribution to the entropy is negative with the total entropy remaining positive, which confirms that a structured phase has lower entropy than an unstructured one.

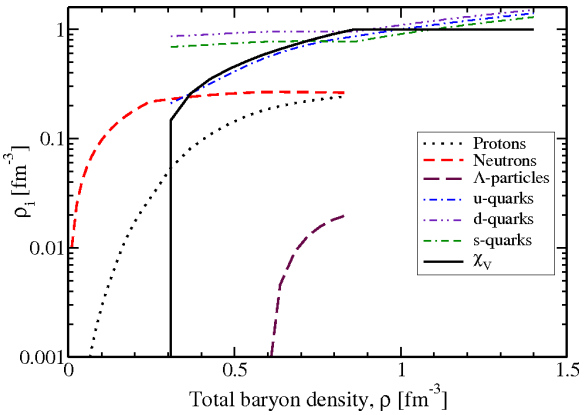

Fig. 1.— Chemical composition of the G_{180}^{300} equation of state as a function of total baryon density. Individual particle densities ρ_i refer to the density in regions filled with the respective phase. χ_v is the (dimensionless) volume fraction of quark matter.

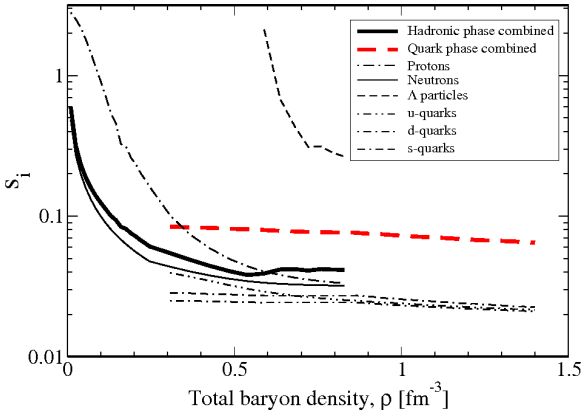

Fig. 2.— Entropy per baryon at $T = 1$ MeV in each phase, $s_{\rm H}$ and $s_{\rm Q}$, and per particle for each particle, s_i, as functions of total baryon density for the G^{300}_{180} equation of state. Protons and Λ particles have high s_i because they are so rare, but contribute little to $s_{\rm H}$ for the same reason.

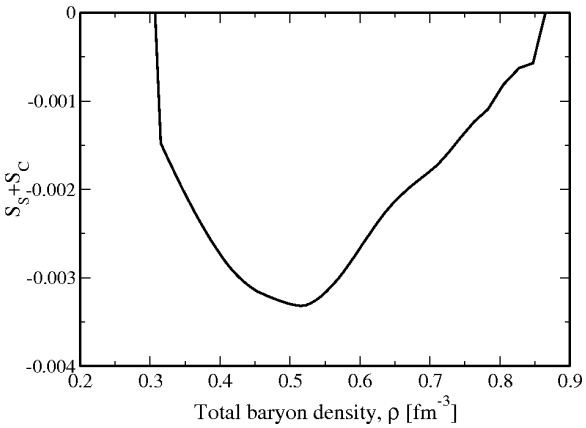

Fig. 3.— Sum of surface and Coulomb entropy as a function of total baryon density for the G^{300}_{180} equation of state at $T = 1$ MeV

We have calculated the structure of a sequence of stars with rotation frequencies (as seen by an observer at infinity) between zero and the limiting mass-shedding Kepler frequency for the G^{300}_{180} equation of state. For this purpose we use the perturbative method of Hartle (1967) and Hartle & Thorne (1968) as implemented in the numerical code developed by Weber which also solves self-consistently for the general relativistic Kepler frequency $\Omega_{\rm K}$ – see Weber (1999) for the derivation of $\Omega_{\rm K}$ and (Weber et al. 1991; Weber & Glendenning 1992) for further details. The sequence has constant total baryon number $A = 1.87 \times 10^{57}$ and nonrotating total gravitational mass $M = 1.42$ M$_\odot$. The Kepler frequency is then found to be $\Omega_{\rm K} = 6168$ rad s^{-1} corresponding to a period of 1.02 ms.

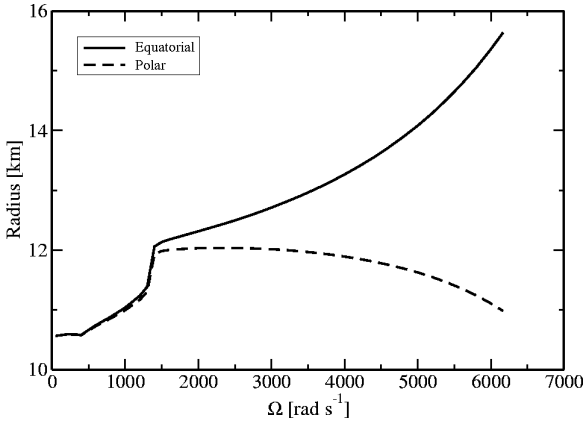

Fig. 4.— Circumferential stellar radius in the equatorial and polar directions for rotating stars of total nonrotating gravitational mass $M = 1.42$ M$_\odot$.

Figs. 4 and 5 show a few properties of the models. The stars are significantly distorted by rotation and increase their equatorial radius at the Kepler frequency by half the nonrotating radius (Fig. 4) while losing the pure quark matter core at $\Omega = 1400$ rad s^{-1} (Fig. 5). Since the stellar photon luminosity is proportional to the surface area and must match the energy flux emerging from the core, higher surface temperatures must also be expected at low rotation frequencies for this reason alone. The distortion from spherical symmetry depends on polar angle, however, and above the frequency at which the quark matter core is lost the star actually contracts in the polar direction.

In Fig. 5 we show the location of the phase boundaries between pure hadronic matter, the various geometries of the mixed phase and the pure quark matter phase. Here we use as the free variable the baryon number, a, contained within a surface on which the density is uniform (i.e spatially but *not* temporally constant). The Eulerian density change $(\mathrm{d}\rho/\mathrm{d}\Omega)_r$ can be positive or negative depending on location while the Lagrangian derivative $(\mathrm{d}\rho/\mathrm{d}\Omega)_a$ is always negative, and so a is a more convenient variable for some purposes. In Fig. 5 borders are shown at the densities which correspond to each transition and a is scaled to the total baryon number, A. We note that a large fraction of the star is converted to quark matter as the star spins down. The pure quark matter core appears below $\Omega = 1400$ rad s^{-1} and grows to eventually comprise 30 % of the stellar gravitational mass and 26 % of the stellar baryon number.

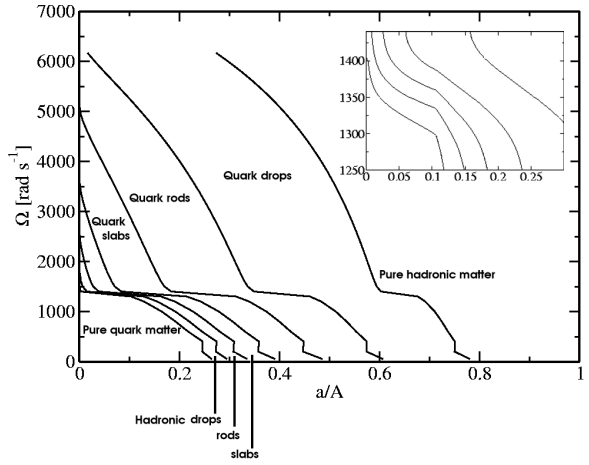

Fig. 5.— Location of phase boundaries in stars of nonrotating mass $M = 1.42$ M$_\odot$. The locations are given as the fractions of the total stellar baryon number contained within a surface of spatially constant density corresponding to each transition. The inset shows the region where the phase boundaries almost – but not quite – cross.

Within the framework of Hartle (1967) the changes in pressure and density with respect to a nonrotating star are second order effects in the rotation frequency, and as discussed by Weber & Glendenning (1992) this remains true even at the limiting Kepler frequency, Ω_K, where the star would shed mass from the equator. The Lagrangian density change during spindown can then be reasonably approximated by the order of magnitude estimate (see also Fernández & Reisenegger (2005))

$$\left(\frac{\partial\rho}{\partial\Omega^2}\right)_{a,A} \sim -\frac{\rho}{\Omega_{\rm K}^2} \qquad (21)$$

Fig. 6 shows how the numerically calculated spin down compression rate compares to this estimate in the mixed phase – we have checked it at other positions as well. For stars with high spin frequencies and no pure quark matter core Eq. (21) is a reasonable approximation although an overestimate in some regions. It is off by approximately a factor of 0.1 below the frequency where the pure quark matter core forms.

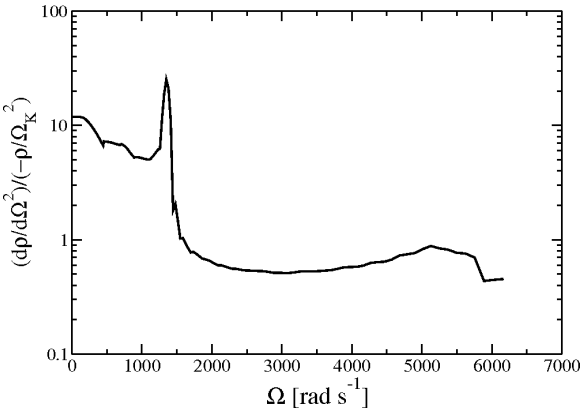

Fig. 6.— Frequency derivative of density scaled to the estimate in Eq. (21) at $a/A = 0.33$ as a function of spin frequency. The estimate is best at high spin frequencies but holds within a factor of 30 in all stars.

Eq. (21) can be used to give a rough estimate of the effects of the additional en-

tropy production related to density change in Eq. (11)

$$T\frac{\mathrm{d}s}{\mathrm{d}t} = \frac{c_{\rm v}}{\rho}\frac{\mathrm{d}T}{\mathrm{d}t} + T\frac{\mathrm{d}s}{\mathrm{d}\rho}\frac{\mathrm{d}\rho}{\mathrm{d}t} \simeq \frac{c_{\rm v}}{\rho}\frac{\mathrm{d}T}{\mathrm{d}t} - T\frac{\mathrm{d}s}{\mathrm{d}\rho}\frac{\rho}{\Omega_{\rm K}^2}\times 2\Omega\dot{\Omega}\ . \quad (22)$$

Taking the entropy per particle from Eq. (13) this implies that the bulk terms in Eq. (11) are of the order of

$$T\frac{\mathrm{d}\rho}{\mathrm{d}t}\frac{\mathrm{d}s}{\mathrm{d}\rho} \simeq \frac{2}{3}\frac{\Omega\dot{\Omega}}{\Omega_{\rm K}^2}Ts \simeq -10^{-15}T_9^2\left(\frac{B}{10^{14}\ \mathrm{G}}\right)^2 \times \left(\frac{\Omega/6000}{\mathrm{rad\ s^{-1}}}\right)^4\left(\frac{\rho}{\mathrm{fm^{-3}}}\right)^{-\frac{1}{3}}\mathrm{erg\ s^{-1}}\ , \quad (23)$$

where we have taken $\Omega_{\rm K} = 6000$ rad s^{-1}, assumed a standard dipole model for the spin-down so $\dot{P} = (B_{19}/3.2)^2P^{-1}$ with the spin period, P, measured in seconds and the magnetic field, B in units of 10^{19} G. As a rough estimate the total heating power from the bulk terms in Eq. (11) in the absence of pairing and for a star of constant density and temperature with a baryon number of 10^{57} is then of the order of

$$W_{\rm Bulk} \sim 10^{42}T_9^2\left(\frac{B}{10^{14}\ \mathrm{G}}\right)^2\left(\frac{\Omega/6000}{\mathrm{rad\ s^{-1}}}\right)^4 \times\left(\frac{\bar{\rho}}{\mathrm{fm^{-3}}}\right)^{-\frac{1}{3}}\mathrm{erg\ s^{-1}}\ . \quad (24)$$

This includes only the bulk terms of Eq. (11), but on general grounds one would expect this to be a reasonable approximation of the total additional entropy production. The latent heat has the same basic origin – the release of entropy with changing density – and is therefore expected to be of the same order of magnitude as the bulk terms in Eq. (24). In the following section we shall find that this is justified under most, but not all, circumstances.

The estimated heating in Eq. (24) is to be compared with the neutrino and photon luminosities which in the absence of pairing phenomena can roughly be estimated as (Page et al. 2006)

$$L_\nu^{\rm slow} \sim 10^{40}T_9^8\ \mathrm{erg\ s^{-1}} \quad (25)$$

$$L_\nu^{\rm fast} \sim 10^{45}T_9^6\ \mathrm{erg\ s^{-1}} \quad (26)$$

$$L_\gamma \sim 10^{33}T_9^2\ \mathrm{erg\ s^{-1}} \quad (27)$$

where 'slow' refers to stars dominated by relatively inefficient neutrino emission processes such as the modified Urca cycle, bremsstrahlung or the pair breaking and formation process while 'fast' refers to stars dominated by the highly efficient direct Urca process.

From Eq. (24) we then see that while it may be possible to find combinations of temperature, magnetic field and rotation frequency for which the additional entropy production dominates, such configurations may be difficult to realize in nature. For instance, in order for the heating term in Eq. (24) to dominate the neutrino luminosities the star must be a hot millisecond magnetar. Such an object would be very short lived if it could be created in nature at all. For the heating term to dominate the photon luminosity – which is the more relevant term at late times and low temperatures – extremely high magnetic fields would again be required assuming a dipole model for the spin down. Such conditions – if they were to be realized – would be very short lived and therefore the more difficult to observe.

From these simple estimates we then expect that the release of entropy related to changing bulk density with spin down, the latent heat of phase transitions and changes in the surface and Coulomb energy of mixed phases (smaller still) will have little impact on the thermal evolution of compact stars and be difficult to observe.

4. Spherical Isothermal Cooling

Estimates cannot replace detailed calculations, and the ones discussed above further ignore all effects of superfluidity, the changing chemical composition and the rapid changes in structure at certain frequencies. We therefore proceed in this section to explore these effects through numerical calculations taking the simplest possible approach to solve the thermal balance in Eq. (4).

4.1. Numerical Setup

Neutron stars are commonly taken to be isothermal after an initial thermal relaxation lasting 10-100 years in the sense that the redshifted temperature $T^\infty = Te^\Phi$ is constant below a thermally insulating layer in the outer crust (Gudmundsson et al. 1983). Since we intend only to investigate the late thermal evolution of neutron stars, and as we do not expect the heating terms discussed here to change the isothermality by disturbing the thermal balance of any part of the star with its surroundings, we shall work within this same approximation. To show the full range of effects, plots in the following also include young stars not expected to be isothermal and our results should only be taken as indicative at such early times.

Assuming the star to be thermally relaxed, so the redshifted temperature $T^\infty = Te^\Phi$ is constant below the outer crust, we then integrate Eq. (4) to get a simplified equation for global thermal balance

$$\frac{dT^\infty}{dt} = \frac{1}{C}\left(W^\infty - L_\nu^\infty - L_\gamma^\infty\right) \qquad (28)$$

with

$$C = \int \mathrm{d}a\, T\frac{\partial s}{\partial T} \qquad (29)$$

$$W^\infty = -\int \mathrm{d}a\, e^\Phi T\frac{\partial s}{\partial \rho}\frac{\partial \rho}{\partial \Omega}\dot{\Omega} \qquad (30)$$

$$L_\nu^\infty = \int \mathrm{d}a\, \frac{\epsilon_\nu}{\rho}e^{2\Phi} \qquad (31)$$

$$L_\gamma^\infty = 4\pi R^2\sigma(T_{\rm S}^{(0)})^4 F(B)e^{2\Phi_s} \qquad (32)$$

$$T_{\rm S_6}^{(0)} = g_{14}^{1/4}[(7\zeta)^{2.25} + (\zeta/3)^{1.25}]^{1/4} \qquad (33)$$

$$\zeta = T_9 - 0.001\, g_{14}^{1/4}\sqrt{7T_9} \qquad (34)$$

where $\epsilon_\nu/\rho = Q_\nu$ is the neutrino emissivity, the surface temperature is given in units of 10^6 K, $T_{\rm S_6} = T_{\rm S}/10^6$ K and $T_{\rm S}^{(0)}$ is surface temperature at zero magnetic field strength. We have used a fit appropriate for iron envelopes to the relation between the surface temperature, $T_{\rm S}$, and the inner temperature below the heat-blanketing envelope, T, in which g_{14} is the surface gravity in units of 10^{14} cm s^{-2} (Potekhin et al. 1997; Potekhin & Yakovlev 2001).

The heat conductivity in the crust, which derives mainly from the motion of electrons, becomes anisotropic in a strong magnetic field (Potekhin & Yakovlev 2001; Geppert et al. 2004). It is slightly enhanced in the direction along the magnetic field lines and strongly suppressed in the direction orthogonal to the field lines. The heat blanketing relation and the surface temperature then becomes nonuniform, $T_{\rm local}(B,\theta,g,T) = T_{\rm S}^{(0)}(g,T)\chi(B,\theta,T)$. The photon luminosity must therefore be found by integrating the locally emerging flux and it will depend on magnetic field strength, $L_\gamma(B) = L_\gamma(0)F(B)$. For this purpose we use the fits given by Potekhin & Yakovlev (2001) for $\chi(B,\theta,T)$ and $F(B)$ in a dipole magnetic field. These are good for magnetic fields below 10^{16} G, interior temperature between 10^7 K and 10^9 K and surface temperature above 10^5 K. $F(B)$ reaches a minimum of ~ 0.7 around $B = 10^{13}$ G and grows to about 2 at

$B = 10^{15}$ G for a star of internal temperature $T = 10^9$ K. The location of the minimum moves to lower magnetic field strength for lower internal temperature and the change in photon luminosity can delay or accelerate the cooling at late times accordingly. The figures in Sect. 4.2 show the effective surface temperature at infinity $T_{\rm S}^{\infty} = T_{\rm S}^{(0)} F(B)^{1/4} e^{\Phi}$. A strong magnetic field in the inner crust can also lead to anisotropic heat flow there (see e.g. Geppert et al. (2004) and Aguilera et al. (2008)), but these effects cannot be included here.

For given assumptions about the neutrino emissivity and superfluid gaps Eq. (28) is solved along with the spin down model to give the surface temperature at infinity as a function of time, rotation frequency and magnetic field strength. At each time step Eqs. (29) to (34) are solved to update the stellar structure at the appropriate rotation frequency.

Our equations of thermal balance assume spherical symmetry. This effectively treats rotation as a perturbation whose only effects are to change the size and chemical composition of the stars and to provide additional terms in the thermal balance. This approach ignores the effects of nonradial heat flows and nonspherical perturbations of the metric which can be significant when the star is not spherically symmetric at very high spin frequencies (see Fig. 4). Two-dimensional cooling calculations are beyond our scope, but they have been performed at constant rotation frequency by Schaab & Weigel (1998) and Miralles et al. (1993). For stars rotating at a large fraction of their Kepler frequency these authors found significant effects on the thermal evolution during the nonisothermal epoch, and polar temperatures up to 31% higher than the equatorial temperatures even for internally isothermal stars. The recent work of Geppert et al. (2004); Aguilera et al. (2008,?) further includes the influence of large magnetic fields in the crust and Joule heating by magnetic field decay in two dimensions. This results in nonradial heat flow and significant heating from magnetic field decay. We focus on the effects of deconfinement during spin down however and shall not pursue these aspects here.

Unless otherwise stated we shall use the equatorial radius in Eqs. (32) to (34). We have performed calculations with the polar radius too and will show one such example. At high rotation frequency the surface temperature is then higher and responds less to changes in rotation frequency. We expect results in a two-dimensional code would be intermediate between these and such a calculation would be a significant improvement on what is presented here. With this in mind we use the equatorial radius to show the most pronounced effects of spin down. However, we also note that the strongest effect we have found from spin down stems from the formation of a pure quark matter core. At the rotation frequency where this happens the polar and equatorial radii are very similar (see Fig. 4) and a spherical approximation is reasonable.

Since the stellar moment of inertia I and radius also change with rotation frequency we modify the spin down model described in the previous section to include such effects. The spin down is then determined by (Glendenning 2000)

$$\dot{\Omega} = -\frac{K}{I}\left[1 + \frac{I'\Omega}{2I}\right]^{-1} \Omega^m, \quad I' = \frac{{\rm d}I}{{\rm d}\Omega} \tag{35}$$

$$K = (2/3) R^6 B^2 \sin^2\alpha \tag{36}$$

where α is the inclination angle between the magnetic axis and the rotation axis and $m-1$ is the multipolarity – usually $m = 3$ for magnetic dipole braking or $m = 5$ for gravitational

quadrupole radiation. We take $\sin^2\alpha = 1$ and use the canonical value $m = 3$ for a dipole spin down.

As for the neutrino emissivities and superfluid properties of the neutron star we are interested in the most important effects only and aim for transparency in the model. In the quark phase we include the direct and modified Urca cycles as well as bremsstrahlung using the emissivities in Blaschke et al. (2000). The *us*-branch of the direct Urca cycle fulfills the triangle inequality,

$$k_{\mathrm{F}_s} < k_{\mathrm{F}_u} + k_{\mathrm{F}_e} \tag{37}$$

where k_{F_i} is the Fermi momentum of the strange-quark, up-quark and electron respectively. It is thus allowed throughout the quark phase, but its *ud*-counterpart is forbidden as it cannot conserve both energy and momentum. This difference stems from the assumed strange quark mass of 150 MeV.

In the hadronic phase we again include the direct and modified Urca cycles as well as bremsstrahlung using the emissivities given in Yakovlev et al. (2001). We ignore the effects of hyperons here because of their low abundance. In neutron stars the direct Urca reaction is often allowed only at very high densities because it cannot fulfill both energy and momentum conservation unless the proton fraction is above the value where both charge neutrality and the triangle inequality can be observed (Lattimer et al. 1991). It is critical to note that this is not so in hybrid stars with a mixed phase. The mixed phase is possible precisely because charge neutrality does not have to be observed locally, and it is favorable because the hadronic phase lowers its nuclear symmetry energy by increasing the proton fraction (Fig. 1). Hence the hadronic direct Urca cycle is active in the mixed phase, and as it is about three orders of magnitude faster than the *us*-branch of the quark direct Urca cycle it controls the cooling of hybrid stars with a mixed phase unless reduced by pairing effects.

Additional neutrino processes should be included in a more sophisticated treatment – particularly in the crust – but as stated above we are mainly interested in the general properties of the additional entropy production and the changing chemical composition and we shall here leave out such terms.

If there is any attractive interaction among particles in a degenerate Fermi system they will pair, and the resulting superfluidity has important consequences for the thermal properties of neutron star matter and the thermal evolution of neutron stars. Pairing in general delays the cooling because it suppresses most of the neutrino emissivities and enhances the heat capacity at temperatures just below the critical. However it also opens additional neutrino emission processes, suppresses the heat capacity far below the critical temperature and enhances the thermal conductivity, and it may therefore also accelerate the cooling at certain epochs (see e.g. Yakovlev et al. (1999) for a detailed account).

There is considerable uncertainty concerning the relevant superfluid phase in quark matter – see Alford et al. (2008) for a comprehensive review of the effects of pairing among quarks and the possible range of phases. For this first investigation of consequences for the thermal evolution of a quark-hadron phase transition during spin down we assume a simplified but physically transparent model for quark matter pairing which essentially corresponds to pairing in the color-flavor locked phase (Alford et al. 1999; Alford 2001). In this model each flavor participates equally, the gap $\Delta_{Q,0}$ is independent of density and the critical temperature is $T_c = 0.72\Delta_{Q,0}$ (see Schmitt et al. (2002)). We shall consider a wide range in $\Delta_{Q,0}$ partly because it is in-

teresting for the present calculation, partly because very low gaps may be realized for high strange quark mass as this implies unequal quark Fermi momenta in the unpaired phase. The color-flavor locked phase is generally understood to be so strongly suppressed in all its thermal properties as to be virtually inert with respect to cooling. Since we shall also consider small gaps and since the latent heat derived from the phase transition depends strongly on pairing in the quark phase this will not always apply here, but for strong quark pairing the thermal evolution is generally controlled by the hadronic phase. We further note that as shown by Jaikumar et al. (2002) (and stressed by Alford et al. (2008)) Goldstone modes and their related neutrino emissivities and heat capacities are not exponentially suppressed, scaling instead as T^{15} and T^3 respectively. They will therefore dominate in color-flavor locked quark matter at low temperatures, but they are exceedingly small and do not influence our results.

The effects of superfluidity relevant for our purpose are that below the critical temperatures it suppresses the neutrino emissivities and entropies of the participating particles while also allowing additional neutrino emission through Cooper pair breaking and formation. The specific heat is enhanced just below the critical temperature and suppressed at lower temperatures. These effects are incorporated through control functions, $R(T, T_c)$, which multiply the relevant quantities. They depend only on the pairing channel, temperature and gap size, and may therefore be calculated given expressions for the gap size momentum dependence.

In the quark matter phase we use the simplest possible control functions and suppress the direct Urca emissivity by a factor of $e^{-\Delta_{\rm Q}/T}$ and the modified Urca and bremsstrahlung emissivity by a factor of $e^{-2\Delta_{\rm Q}/T}$, where (following Steiner et al. (2002)) $\Delta_{\rm Q} = \Delta_{Q,0}\sqrt{1-(T/T_c)^2}$ is the pairing gap at the local temperature, $T = T^{\infty}e^{-\Phi}$.

The specific heat and entropy of superfluid particles are also modified at temperatures below the critical temperature. In the quark matter phase we use the fit to the ${}^1S_0$ control function for the specific heat given by Yakovlev et al. (1999). We further fit the results of Mühlschlegel (1959) for the entropy suppression to obtain

$$s_{\rm sf} = 0.95\, s_0 \times (T/T_{\rm c}) e^{-T_{\rm c}/T} \times \left[0.43 + 3.82(T/T_{\rm c}) - 1.41\,(T/T_{\rm c})^2\right]. \quad (38)$$

Where s_0 is the nonsuperfluid entropy. This expression is applied to reduce the entropy of both quarks and hadrons (thus here neglecting the difference between different pairing states of neutrons). The entropy difference between the superfluid and the normal phase depends on temperature as $\Delta s \propto -(1 - T/T_{\rm c})$ close to the critical temperature (Landau & Lifshitz 1980) with s_0 becoming negligible below $0.2T_{\rm c}$. This has the effect of gradually turning the latent heat in Eq. (11) from a cooling term into a heating term, but it also suppresses the bulk terms in Eq. (11).

In the absence of detailed calculations of control functions for the entropy of superfluid quark matter phases in the literature we have employed Eq. (38) in the quark matter phase though it is strictly relevant only for BCS superfluidity. Eq. (38) is, however, consistent with the exponential suppression of entropy below the critical temperature which would be expected in any such calculation, and we do not expect that our results are sensitive to this choice.

Pairing further opens the important possibility of neutrino emission by Cooper pair breaking and formation in the quark phase

and we include the associated emissivity as described in Jaikumar & Prakash (2001) using the fit to the $^1S_0$ control function in Yakovlev et al. (1999).

Among the nucleons pairing is predicted for neutrons in the $^1\mathrm{S}_0$ and $^3\mathrm{P}_2$ channels and for protons in the $^1\mathrm{S}_0$ channel. The gaps can be calculated self-consistently but results are uncertain and vary greatly both in terms of the maximum gap size and in terms of density dependence – see e.g. Lombardo & Schulze (2001); Page et al. (2004, 2006) for collections of these results. We shall here use gaps with a phenomenological momentum dependence as suggested by Kaminker et al. (2001), Andersson et al. (2005) and recently Aguilera et al. (2008)

$$\Delta(k_{F,N}) = \Delta_0 \frac{(k_{F,N}-k_0)^2}{(k_{F,N}-k_0)^2+k_1^2} \tag{39}$$

$$\times \frac{(k_{F,N}-k_2)^2}{(k_{F,N}-k_2)^2+k_3^2} \tag{40}$$

where $k_{F,N}$ is the Fermi momentum of the relevant nucleon, $N = n, p$. Our choices for the parameters Δ_0 and k_i correspond to sets a, e and h of Aguilera et al. (2008) (see that work for references to the model calculation underlying these fits). Eq. (40) is valid only in the range $k_0 < k < k_2$ with $\Delta(k_{F,N}) = 0$ outside this range, and where the gaps for $^1\mathrm{S}_0$ and $^3\mathrm{P}_2$ pairing of neutrons are both nonzero we use the largest of the two gaps. We further use the relations between critical temperature and pairing gap listed by Yakovlev et al. (1999).

In the hadronic phase neutrons and protons may pair simultaneously in different channels and so the resulting calculations for the control functions can be quite involved. We use the fits to numerically calculated control functions for each process and each pairing channel compiled in Yakovlev et al. (1999) (or Yakovlev et al. (2001) – see these works for detailed references). Where protons and neutrons pair simultaneously we use the combined factors listed in these works if available and if not then the smallest of the two independent control functions.

The hadronic pair breaking and formation process can be very powerful and may dominate the thermal evolution when pairing first sets in, but it was recently shown by Leinson & Pérez (2006) to be strongly suppressed in the singlet state channel by approximately a factor of 10^{-6} relative to the $^3\mathrm{P}_2$ channel (see also the recent work of Steiner & Reddy (2009)). In the hadronic phase we therefore include pair breaking and formation only for neutrons at high densities where they pair in the $^3\mathrm{P}_2$ channel and for this we again use the emissivity and control function given in Yakovlev et al. (1999, 2001).

4.2. Numerical Results

Figures 7 to 12 explore consequences for the thermal history of hybrid stars of including time dependent structure and entropy production by spin down compression in the cooling calculations with the approximations discussed above. They show the surface temperature and additional entropy production at infinity as functions of time, magnetic field and quark pairing gap energy.

In Fig. 7 we show the thermal evolution of stars with quark pairing gap $\Delta_{Q,0} = 10$ MeV, a range of magnetic fields and initial spin period around 1 ms. The extremely rapid initial rotation is interesting because it means the stars start out with no pure quark matter core and undergo drastic changes in structure as a pure quark matter core develops around $\Omega = 1400$ rad s^{-1}. We see this in Fig. 7 as a short period of increasing temperature at the time corresponding to this angular velocity for a given magnetic field. During this short period the heating term from the addi-

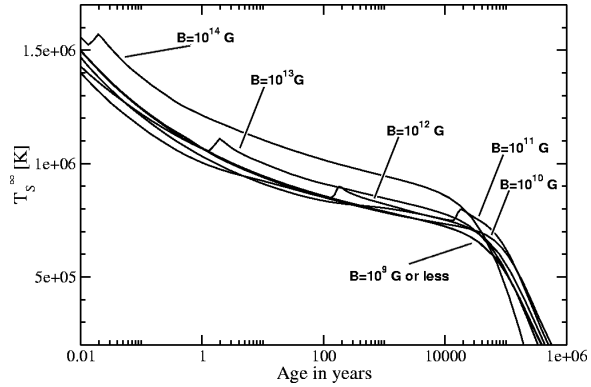

Fig. 7.— The effect of spin down compression on cooling curves for stars with initial spin frequency $\Omega_{\rm start} = 6000$ rad s^{-1} and constant magnetic field as labeled for each curve. The quark core is assumed superconducting with $\Delta_{Q,0} = 10$ MeV. The increasing quark matter fraction produces slower cooling and a jump in temperature with the appearance of the pure quark matter phase.

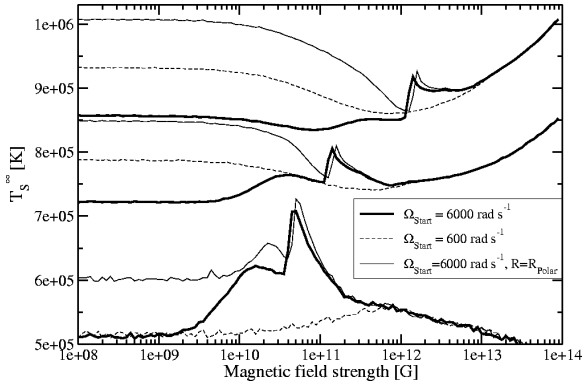

Fig. 8.— Variation of surface temperature at infinity with magnetic field for stars at ages 10^2, 10^4 and 10^5 years from above. Thick lines have initial spin frequency $\Omega_{\rm start} = 6000$ rad s^{-1} while thin dashed lines start with $\Omega_{\rm start} = 600$ rad s^{-1}. Thin continuous lines use the polar rather than the equatorial radius. The quark core is assumed superconducting with $\Delta_{Q,0} = 10$ MeV. We note a slow increase in temperature for old stars and a sudden jump at the magnetic field corresponding to significant spin down at specific ages. The suppression in temperature at low magnetic field and increase at high field is due to the effects of the magnetic field of the heat blanketing relation.

tional entropy production actually dominates which is shown in more detail in Fig. 10 discussed below. Further, the changing neutrino emissivity and heat capacity with the introduction of more quarks in the star and the reduction in stellar surface area as the pure quark matter core develops all affect the thermal evolution. This implies somewhat slower cooling – with our specific choice of parameters – and higher surface temperature. For the internal temperature, T, we have found essentially a transition between two otherwise similar cooling tracks; one for stars with no pure quark matter core and one for stars with a fully developed quark matter core. The effective surface temperature also depends on magnetic field strength through $F(B)$ however. For this reason such an easy interpretation is difficult from Fig. 7 alone.

The magnetic field strength determines the spin down and affects the heat blanketing relation. Fig. 8 shows how the temperature varies at specific ages with the magnetic field strength (which is kept constant in time itself). This is shown for initial spin frequencies of 6000 rad s^{-1} and 600 rad s^{-1} and using the polar radius in addition to the equatorial when calculating the surface temperature.

For low initial spin frequency we find no significant effects of spin down in Fig. 8. The change in temperature at a specific age with increasing magnetic field is due to the effects of the magnetic field on the heat blanketing relation and photon luminosity. If these effects were left out the curves for low initial spin frequency would be almost constant.

If the initial rotation frequency is sufficiently high to exclude the pure quark matter phase it is a different matter. A strong magnetic field initially suppresses the surface temperature of young stars with high rotation frequencies, but it then gives a sharp jump at the magnetic field strength which ensures that a pure quark matter core is formed at a particular age. For older stars there is also a slight increase in surface temperature before the formation of a pure quark matter core when the equatorial radius is used. If the effects of the magnetic field on the heat blanketing relation were left out the curves at high initial spin frequency become nearly constant for $B > 10^{13}$ G and for fields too weak for spin down to set in at the particular age. In this case there would still be a jump in temperature at the magnetic field strength corresponding to formation of a pure quark matter core for a specific age however.

Replacing the equatorial radius with the polar in Eqs. (32) and (34) (thin continuous lines in Fig. 8) we find higher surface temperatures before the introduction of pure quark matter in the core and still a clear jump in temperature after. The gradual increase in temperature before the jump found in the other curves is absent except for old stars. This can be understood if we remember that the polar radius is smaller than the equatorial and less sensitive to spin down at high rotation frequencies. We have checked that a similar pattern may be seen in plots of temperature versus time using the polar radius. We expect that full two-dimensional calculations would give results which are at high rotation frequencies intermediate between what we have found using a spherical approximation. The similarity between curves with polar and equatorial radius at the jump in temperature shows that our calculations are insensitive to the approximation at the spin frequency where the pure quark matter core forms and where we find the strongest effect of spin down.

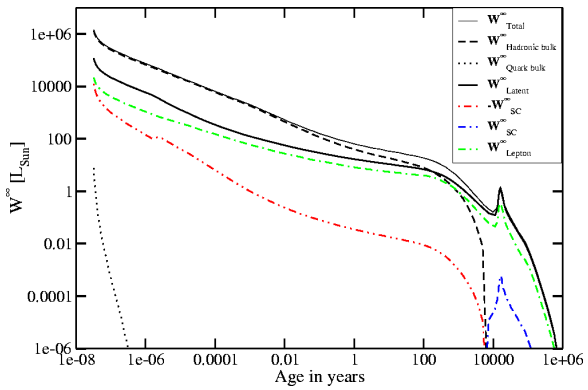

Fig. 9.— Numerical value of the entropy production as defined in Eq. (30) as a function of time for a star with magnetic field $B = 10^{11}$ G and quark pairing gap $\Delta_{Q,0} = 10$ MeV. $W_{\rm Tot}$ is split into contributions with different physical origins as explained in the text. The surface and Coulomb term changes sign and the negative of this term is shown as well. The latent heat and bulk terms are dominant, and the spike is caused by the appearance of a pure quark matter phase.

In Figs. 9 and 10 we explore the importance of the heating term in a little more detail. Fig. 9 shows the numerical value of W^∞ and its various contributions as a function of time for a star with pairing gap $\Delta_{Q,0} = 10$ MeV and magnetic field $B = 10^{11}$ G. The total entropy production, W^∞, is split into contributions corresponding to (integrals of) the terms in Eq. (11). $W^\infty_{\rm Latent}$ corresponds to the latent heat, $W^\infty_{\rm Hadronic\ bulk}$ to the hadronic bulk term, $W^\infty_{\rm Quark\ bulk}$ to the quark bulk term and $W^\infty_{\rm SC}$ to the surface and Coulomb term of Eq. (11). Leptons do not participate in the deconfinement transition, so their entropy is assumed continuous across the phase boundary. They are separated from the other particles in the form of $W^\infty_{\rm Lepton}$ in Fig. 9.

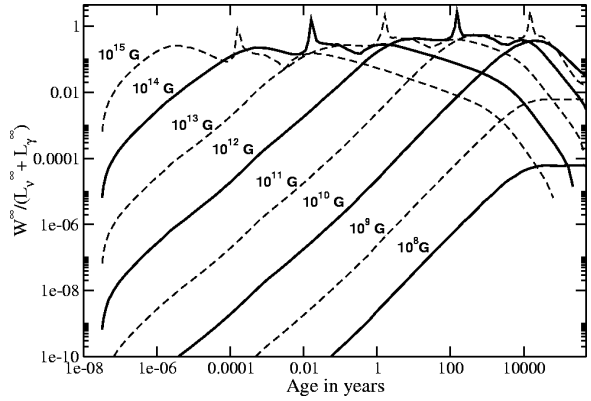

Fig. 10.— The total entropy production scaled to the combined neutrino and photon luminosity for stars with quark paring gap $\Delta_{Q,0} = 10$ MeV and magnetic fields as indicated just above each curve. The different line styles are meant only to help guide the eye. Note that at the peaks reaching above 1 the entropy production actually dominates the cooling terms and the temperature increases. Also note that this is only possible for stars changing structure rapidly with the introduction of a pure quark matter core.

The bulk and lepton contributions always act as heating terms while the surface and Coulomb term changes sign and turns into a heating term with the onset of hadronic superfluidity around age 4000 years with the hadronic bulk term simultaneously falling away. The quark bulk term is very small because for a pairing gap of 10 MeV the quark matter is strongly superconducting at all times except the very early and the quark entropy is therefore suppressed. This also implies, however, that hadrons making the transition across the phase boundary essentially release all their entropy, and so the latent heat, which changes sign and becomes a heating term with the onset of quark superfluidity, is therefore quite significant and actually comes to dominate around the time when the hadronic bulk term falls away. The lepton term and the surface and Coulomb term are relatively small but significant when the bulk terms are eliminated through the onset of pairing. The peak in the total around age 20000 years corresponds to the appearance of a pure quark matter phase in the core and the ensuing rapid changes in structure, and it contributes to produce the short interval of increasing temperature seen in Fig. 7.

Fig. 10 shows the total entropy production scaled to the total neutrino and photon luminosity, $W^{\infty}/(L_{\gamma}^{\infty} + L_{\nu}^{\infty})$, for the same set of parameters which gave the cooling curves in Fig. 7. The strong temperature dependence of the neutrino and photon luminosities ensures that the scaled heating term does not increase above unity where heating and cooling exactly balance – except at the peaks caused by the appearance of a pure quark matter core. We also note that as in Fig. 7 the magnetic field must be above $\sim 10^9$ G for W^{∞} to have any discernible effects.

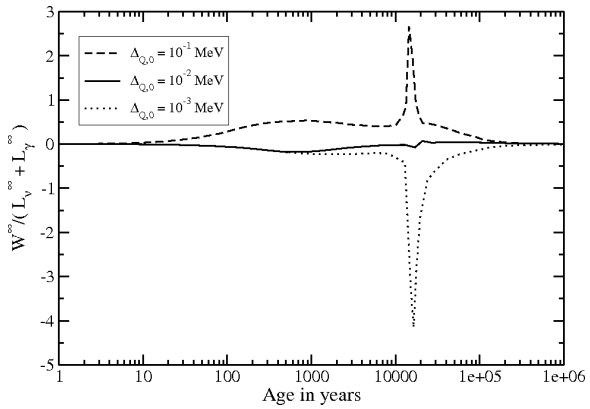

Fig. 11.— The total entropy production scaled to the combined neutrino and photon luminosity for stars with quark paring gap as indicated in the legend and $\Omega_{\rm start} = 6000$ rad s^{-1}. The magnetic field is constant at 10^{11} G. The entropy production changes sign and becomes negative for low pairing gaps and thus acts as a powerful cooling term during some epochs.

While the latent heat for a transition to a strongly superfluid core is a heating term, the transition to a nonsuperfluid core with higher entropy per baryon cools the star. This is illustrated in Fig. 11 where we plot the total heating term scaled to the combined neutrino and photon luminosities at constant magnetic field for a range of quark pairing gaps $\Delta_{Q,0}$. Here we see how the entropy production changes from a heating term to a cooling term and may be quite dominant at certain times depending on the choice of stellar parameters. This can also be observed in Fig. 12 where we plot surface temperature versus age with constant magnetic field for a range of quark pairing gaps. The onset of superfluidity initially delays the cooling and then accelerates it. When the pure quark matter core forms there is a drop in temperature for very low pairing gaps and a jump for high pairing gaps. In fact, however, the major differences between the curves in Fig. 12 are due to the differences in the thermal evolution of superfluid and nonsuperfluid quark matter rather than spin down related effects. Old stars with a nonsuperfluid quark matter core cool more slowly than those without a quark matter core.

A rich picture has now emerged from the coupling between the thermal evolution and spin down compression with deconfinement. The spin down may change the thermal evolution of hybrid stars by heating and cooling them at various ages and by changing the structure and chemical composition – or it may be entirely inconsequential depending on quark superfluidity and initial spin frequency. The effects we found turned out to depend strongly on the inclusion of quark pairing and the timing of the appearance of the pure quark matter phase in the stellar core. These are subject to the specific assumptions made concerning the equation of state, stellar baryon number and pairing regime, so it is essential to

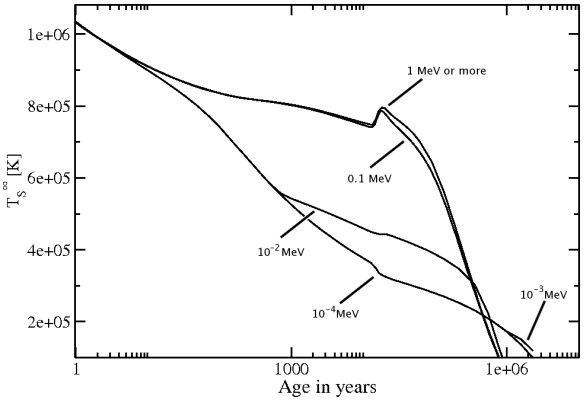

Fig. 12.— The effect of spin down compression on cooling curves for stars with initial spin frequency $\Omega_{\rm start} = 6000$ rad s^{-1} and quark pairing gap $\Delta_{Q,0}$ as labelled for each curve. The magnetic field is constant at 10^{11} G

stress that the results discussed in the present section illustrate the general point that spin down and thermal cooling may be interdependent, rather than providing quantitatively reliable predictions.

Bearing this in mind we show in Fig. 13 how calculations for selected pairing gaps and magnetic field strengths measure up to observational data on the thermal state of isolated neutron stars (kindly supplied by Dany Page). This figure is shown partly as a consistency check for our calculations and partly to compare the size of the effects we have found with the accuracy of actual measurements. We stress that the observational data are consistent with static cooling models (Page et al. 2004) and that we do not suggest that the effects of spin down are necessary to explain them. Further the effects we have found occur after thermal relaxation only for magnetic field strength below $\sim 10^{12}$ G. For those sources in Fig. 13 for which the field is known it is above that value (Pons et al. 2007).

Fig. 13 explores a range of quark pairing

gaps which in our pairing scheme are density independent. In nature the pairing gap would not span a range this broad, but it could be density dependent and variations between stars in mass and density would then introduce variations in their thermal evolution. Similarly stars with different masses would have a different phase structure and acquire pure quark matter cores at different rotational frequencies thus further complicating the picture.

Because the hadronic direct Urca mechanism and the neutron pair breaking and formation mechanism are active in the mixed phase our models are consistent only with the cold sources and the effects of spin down do not change this conclusion. That these mechanisms are the cause of the generally low temperatures in our models can be seen if they are artificially left out. The two dotted lines in Fig. 13 show – for illustration only – that temperatures are much higher if these mechanisms are suppressed. Such a suppression could occur for certain quark pairing schemes where pairing forces the quark phase to become electrically neutral or positive rather than negative, thereby reducing the proton content in the hadronic phase below the threshold for direct Urca. A self-consistent inclusion of such effects are beyond the scope of the present investigation. We stress again that the inconsistency with hot sources seen in this figure is subject to the choice of stellar and thermal models made for the specific purpose of studying the effects of deconfinement during spin down. Thus it should not be seen as indicating a general breakdown in cooling theory.

The true signal of deconfinement we have found is in the transition between cooling curves with and without pure quark matter cores, and in the brief period of increasing or rapidly decreasing temperatures thus caused for certain stellar parameters. As can be seen in Fig. 13 the change in surface temperature caused by deconfinement is smaller than the error bars on the observational data and it will be difficult to test observationally on the basis of data relating only temperature and time.

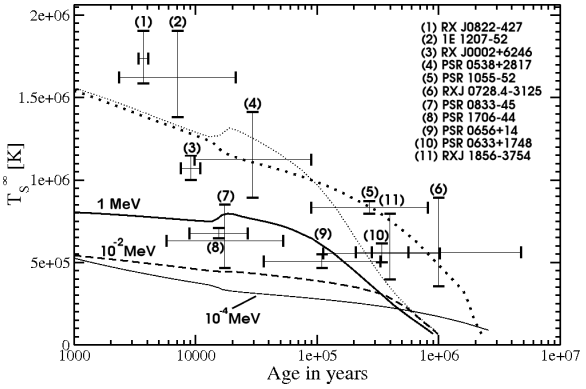

Fig. 13.— Comparison between observational data and cooling calculations with spin down. The stars have initial spin frequency $\Omega_{\rm start} = 6000$ rad s^{-1}, magnetic field strength $B = 10^{11}$ G and quark pairing gaps as indicated. The observational data can be found in Page et al. (2004) and sources are identified by numbers right above or below their temperature error bars. The two dotted lines illustrate slow cooling with artificial suppression of neutrino emission by direct Urca and neutron pair breaking and formation. They have $\Delta_{Q,0} = 10$ MeV (thick line) and 0.01 MeV (thin line). Including these mechanisms only cold sources can be explained. The jump in temperature at the formation of a pure quark matter core is smaller than the error bars on the observational data.

5. Discussion

Our intention with the present work was to explore a possible connection between the spin down and thermal cooling of hybrid stars with a deconfined quark matter core – the appearance of which might be expected to influence theoretical cooling tracks. Specifically

we were interested in the latent heat of the phase transition and the drastic changes in structure and chemical composition resulting from the increasing density with spin down. The general formalism worked out in Sect. 2 would also be relevant to models with no phase transition, however, as the bulk terms in the spin down derived entropy production might also be important in such cases. While estimates of the importance of the spin down derived entropy production did not give cause to expect strong signals of deconfinement in the thermal evolution, numerical calculations revealed clear effects of the changes caused by the appearance of a pure quark matter core. This signature is related to changes in radius, chemical composition, structure and under certain circumstances the additional entropy production both in bulk and in the form of latent heat.

Our numerical work was carried out using a sophisticated and reliable code with respect to the stellar structure solving Hartles perturbative equations for the structure of rotating compact stars self-consistently. The thermal evolution, however, was treated in a spherical isothermal approximation with a somewhat ad hoc approach to the treatment of superfluid pairing in the quark matter phase. Still we believe our work is sufficiently detailed to demonstrate the general point that important signals may be derived from the interplay between spin down and cooling of compact stars, which could in the long run help answer pressing questions about the state of matter at high densities. The signals we have found do not dominate the general thermal evolution of hybrid stars but they do complement the standard picture. By correlating temperature with magnetic field strength and spin frequency they may also help break the degeneracy between models relating only temperature and time.

The signature of deconfinement found here is below the present observational sensitivity and not of sufficient strength to set apart the cooling curves with temperature versus time for hybrid stars. The correlation between temperature and magnetic field strength provides a possible alternative. To test such a correlation it would be necessary to obtain accurate temperatures for a number of stars of approximately the same age for which the spin down could also be detected by the emission of pulses in either radio or X-ray. It might then be possible to test for features in the relation between temperature and magnetic field – or equally interesting, the rotation frequency itself – which as demonstrated here could result from a strong phase transition if the initial rotation frequency was sufficiently high to have spun out the high density phase.

Contemplating these prospects it is important to consider that alternative effects not treated here might determine the relation between spin down and thermal evolution. Most pressingly the heat from magnetic field decay was employed by Pons et al. (2007) to explain the observed correlation between temperature and magnetic field and it may well drown out any other effects – although as noted by the authors the magnetic field decay itself has not yet been independently demonstrated. Recent work by Aguilera et al. (2008) and Aguilera et al. (2008) on the cooling of magnetized neutron stars in two dimensions also highlighted the importance of the magnetic field strength, geometry and possible decay for the thermal evolution of neutron stars. These authors find strongly anisotropic surface temperature distributions and possibly an inverted temperature distribution with hot equatorial regions for middle aged stars. They further show that the effects of magnetic field decay and Joule heating can dominate the thermal evolution at strong and interme-

diate field strengths – even to the point that the effects of the direct Urca process may be hidden by this heating term in magnetars.

The work of Reisenegger (1995) and Fernández & Reisenegger (2005) is also most important. These authors consider the second term on the right hand side of Eq. (4) which is shown to give rise to so-called roto-chemical heating as the weak interactions required to maintain chemical equilibrium are unable to keep pace with the increasing density. Fernández & Reisenegger (2005) found that old millisecond pulsars reach a quasi-equilibrium in which the photon luminosity is determined entirely by the spin down power and remains much higher than otherwise attainable. Their work considered only nucleonic equations of state but similar results should clearly be expected for hybrid stars just as part of the effects demonstrated here should be expected to show up in nucleonic stars.

Given the possible importance of such alternatives and the shortcomings of the present study discussed above, a more complete treatment of the interplay between the spin down and thermal evolution of neutron stars seems desirable before strong assertions can be made concerning the specific shape of cooling tracks. As well as including all possible energy sources and sinks this should be extended to consider a wider range of stellar masses, equations of state, phase transitions and pairing regimes. A two dimensional code could further treat the influence of the magnetic field on heat flows in the inner crust and the effects of nonspherical heat flows for rotationally perturbed stars – aspects which are all independently well described in the literature.

It should further be noted that the rotation frequency at which the pure quark matter core appears depends strongly on the stellar baryon number and the equation of state, and it may well be lower than discussed here thus changing the timing of spin down related effects. The strongest signature of deconfinement found here depends entirely on the formation of a pure quark matter core where none existed previously. If, on the other hand, a pure quark matter phase is present in the core of stars at even the highest rotation frequencies – as is the case for other equations of state – we would not expect equally strong signals from deconfinement with spin down compression.

It is possible that circumstances not considered here could provide a more pronounced link between rotation and cooling. If for instance the magnetic field varies over time – and as discussed by Geppert (2006) this may well be the case – the timing of any strengthening or decay of the magnetic field may provide entirely different spin down histories. Alternatively the temperature of stars being spun up in accreting binaries should to some extent be determined by the changing chemical composition and this could provide an alternative approach.

Additional energy release would also be expected if the phase transition cannot maintain thermodynamic or hydrostatic equilibrium as was assumed here. As the most extreme example of this, we have entirely ignored the instabilities and corequakes which might accompany the appearance of a pure quark matter phase in a star far from equilibrium (Zdunik et al. 2006). Such events could release large amounts of energy and significantly change the thermal evolution by reheating the star.

While many essential issues thus remain poorly explored we hope to have demonstrated the possible usefulness of considering the connection between the spin down and thermal evolution of neutron stars. Although the results of such work may not be imme-

diately applicable to observational tests, we believe they could prove most valuable in the long run.

We wish to acknowledge helpful conversation with Sanjay Reddy on the hadronic pair breaking and formation process and to thank Dany Page for the use of his compilation of observational data. We are also grateful to Dima Yakovlev and Oleg Gnedin for providing us with an earlier version of their cooling code, which we took advantage of when developing the code used for this study.
M. Stejner wishes to thank San Diego State University for its hospitality during part of this work.
The research of F. Weber is supported by the National Science Foundation under Grant PHY-0457329, and by the Research Corporation.
J. Madsen is supported by the Danish Natural Science Research Council.

A. Appendix A, Derivation of the Energy Balance in Mixed Phases

To derive Eq. (4) from Eq. (1) we proceed analogously to Thorne (1966) and Weber (1999) but work in terms of baryon number a instead of radial coordinate. We first define the nuclear energy generation rate per baryon as the rate, q, at which rest mass is converted to internal energy as measured by an observer in the shell and at rest with respect to the shells reference frame

$$q = -\frac{\mathrm{d}\bar{m}_{\mathrm{B}}}{\mathrm{d}(\text{proper time})} = -\frac{\mathrm{d}\bar{m}_{\mathrm{B}}}{e^{\Phi}\mathrm{d}t}\,, \tag{A1}$$

where $\bar{m}_{\mathrm{B}}$ is the average rest mass per baryon and we work in units with. The first term on the right hand side of Eq. (1) is the amount of rest mass converted to internal energy in the entire shell which is then $q\delta a e^{\Phi}\mathrm{d}t$.

Next we note that by expressing the shells volume in terms of its particle density, $V = (V/\delta a)\delta a = \rho/\delta a$, the second term in Eq. (1) can be written

$$\mathrm{d}W = -P\mathrm{d}\left(\frac{1}{\rho}\delta a\right) + \alpha \mathrm{d}\mathbb{S} + \mathrm{d}E_{\mathrm{C}} \tag{A2}$$

The third term represents the difference between the rates at which energy enters and leaves the shell by radiative or conductive means as measured by an observer in the shell and at rest with respect to the shells reference frame, which may be written

$$\begin{aligned} L_{\mathrm{tot}}(a+\delta a)e^{2(\Phi(a+\delta a)-\Phi(a))} - L_{\mathrm{tot}}(a) &= L_{\mathrm{tot}}(a+\delta a)\left(1 + 2\frac{\mathrm{d}\Phi}{\mathrm{d}a}\delta a\right) - L_{\mathrm{tot}}(a) \\ &= \left(\frac{\mathrm{d}L_{\mathrm{tot}}}{\mathrm{d}a} + 2L_{\mathrm{tot}}\frac{\mathrm{d}\Phi}{\mathrm{d}a}\right)\delta a \\ &= \frac{\mathrm{d}}{\mathrm{d}a}\left(L_{\mathrm{tot}}e^{2\Phi}\right)e^{-2\Phi}\delta a \end{aligned} \tag{A3}$$

and the energy change during a coordinate time interval, $\mathrm{d}t$, is this times the proper time interval $e^{\Phi}\mathrm{d}t$. The two factors of $e^{\Phi(a+\delta a)-\Phi(a)}$ account for redshift and time dilation, respectively, as the energy crosses from the inner to the outer edge of the shell, and we expanded the exponential to order $\mathcal{O}(\delta a)$ as

$$e^{2(\Phi(a+\delta a)-\Phi(a))} \approx 1 + 2[\Phi(a+\delta a) - \Phi(a)] = 1 + 2\frac{\mathrm{d}\Phi}{\mathrm{d}a}\delta a. \tag{A4}$$

Using Eqs. (A1), (A2) and (A3) in Eq. (1) and expressing the change in internal energy in terms of the density of internal energy, $\mathcal{E}_{\mathrm{int}}$, local energy balance can then be written as

$$\mathrm{d}\left(\frac{\mathcal{E}_{\mathrm{int}}}{\rho}\delta a\right) = qe^{\Phi}\delta a\mathrm{d}t - P\mathrm{d}\left(\frac{1}{\rho}\delta a\right) + \alpha\mathrm{d}\mathbb{S} + \mathrm{d}E_{\mathrm{C}} - \left[\frac{\mathrm{d}}{\mathrm{d}a}\left(L_{\mathrm{tot}}e^{2\Phi}\right)\right]e^{-\Phi}\delta a\mathrm{d}t\,. \tag{A5}$$

Rearranging and noting that δa is constant in time we then get the gradient of L_{tot}

$$\begin{aligned} \frac{\mathrm{d}}{\mathrm{d}a}\left(L_{\mathrm{tot}}e^{2\Phi}\right) = e^{2\Phi}\Bigg\{q + \Bigg[&\frac{Pe^{-\Phi}}{\rho^2}\frac{\mathrm{d}\rho}{\mathrm{d}t} + \frac{\alpha e^{-\Phi}}{\delta a}\frac{\mathrm{d}\mathbb{S}}{\mathrm{d}t} \\ &+ \frac{e^{-\phi}}{\delta a}\frac{\mathrm{d}E_{\mathrm{C}}}{\mathrm{d}t} - e^{-\Phi}\frac{\mathrm{d}}{\mathrm{d}t}\left(\frac{\mathcal{E}_{\mathrm{int}}}{\rho}\right)\Bigg]_{a=\text{constant}}\Bigg\} \end{aligned} \tag{A6}$$

Eq. (A6) is the relation we sought giving the luminosity gradient for stars with variable structure and including the contributions from surface and Coulomb terms in the energy density. It may be considerably simplified however by noting that we can write the internal energy density in terms of the total energy density as $\mathcal{E}_{\rm int}/\rho = \epsilon/\rho - \bar{m}_{\rm B}$ in which case from the definition of q

$$q - e^{-\Phi}\frac{\mathrm{d}}{\mathrm{d}t}\left(\frac{\mathcal{E}_{\rm int}}{\rho}\right) = -\frac{e^{-\Phi}}{\rho}\left[\frac{\mathrm{d}\epsilon}{\mathrm{d}t} - \frac{\epsilon}{\rho}\frac{\mathrm{d}\rho}{\mathrm{d}t}\right] . \tag{A7}$$

Inserting this in Eq. (A6) and using the first law as written in Eq. (3) finally gives the expression

$$\begin{aligned}\frac{\mathrm{d}}{\mathrm{d}a}\left(L_{\rm tot}e^{2\Phi}\right) &= -\frac{e^{\Phi}}{\rho}\left[\frac{\mathrm{d}\epsilon}{\mathrm{d}t} - \frac{\epsilon+P}{\rho}\frac{\mathrm{d}\rho}{\mathrm{d}t} - \rho\frac{\alpha}{\delta a}\frac{\mathrm{d}\mathbb{S}}{\mathrm{d}t} - \rho\frac{1}{\delta a}\frac{\mathrm{d}E_{\rm C}}{\mathrm{d}t}\right]_{a=\text{constant}} &\text{(A8)}\\ &= -e^{\Phi}\left[T\frac{\mathrm{d}s}{\mathrm{d}t} + \sum_k \mu_k\frac{\mathrm{d}Y_k}{\mathrm{d}t}\right]_{a=\text{constant}} . &\text{(A9)}\end{aligned}$$

In this discussion we have used baryon number as the independent variable to emphasize the importance of a Lagrangian description for stars with variable structure. This is of course not required for all applications and for comparison with other discussions we note that our expressions can be converted to use radial coordinate as the independent coordinate through the standard relation

$$\mathrm{d}a = 4\pi r^2\rho\left(1 - \frac{2m}{r}\right)^{-\frac{1}{2}}\mathrm{d}r \tag{A10}$$

REFERENCES

Aguilera, D. N., Pons, J. A., & Miralles, J. A. 2008, A&A, 486, 255

Aguilera, D. N., Pons, J. A., & Miralles, J. A. 2008, ApJ, 673, L167

Alford, M. 2001, Annual Review of Nuclear and Particle Science, 51, 131

Alford, M., Rajagopal, K., & Wilczek, F. 1999, Nuclear Physics B, 537, 443

Alford, M. G., Rajagopal, K., Schaefer, T., & Schmitt, A. 2008, Reviews of Modern Physics, 80, 1455

Andersson, N., Comer, G. L., & Glampedakis, K. 2005, Nuclear Physics A, 763, 212

Baldo, M., Burgio, G. F., & Schulze, H. . 2003, [ArXiv:astro-ph/0312446]

Baym, G. 2007, AIP Conference Proceedings, 892, 8

Berger, M. S. & Jaffe, R. L. 1987, Phys. Rev. C, 35, 213

Blaschke, D., Klähn, T., & Voskresensky, D. N. 2000, ApJ, 533, 406

Drago, A., Pagliara, G., & Parenti, I. 2008, ApJ, 678, L117

Endo, T., Maruyama, T., Chiba, S., & Tatsumi, T. 2006, Progress of Theoretical Physics, 115, 337

Fernández, R. & Reisenegger, A. 2005, ApJ, 625, 291

Freire, P. C. C. 2008, AIP Conference Proceedings, 983, 459

Freire, P. C. C., Ransom, S. M., Bégin, S., et al. 2008a, ApJ, 675, 670

Freire, P. C. C., Ransom, S. M., Bégin, S., et al. 2008b, in American Institute of Physics Conference Series, Vol. 983, 40 Years of Pulsars: Millisecond Pulsars, Magnetars and More, ed. C. Bassa, Z. Wang, A. Cumming, & V. M. Kaspi (Melville: AIP), 604

Geppert, U. 2006, [ArXiv:astro-ph/0611708]

Geppert, U., Küker, M., & Page, D. 2004, A&A, 426, 267

Glendenning, N. K. 1990, Nuclear Physics A, 512, 737

Glendenning, N. K. 1992, Phys. Rev. D, 46, 1274

Glendenning, N. K. 2000, Compact stars : nuclear physics, particle physics, and general relativity (Berlin: Springer)

Glendenning, N. K. & Weber, F. 2001, ApJ, 559, L119

Gudmundsson, E. H., Pethick, C. J., & Epstein, R. I. 1983, ApJ, 272, 286

Hartle, J. B. 1967, ApJ, 150, 1005

Hartle, J. B. & Thorne, K. S. 1968, ApJ, 153, 807

Heiselberg, H., Pethick, C. J., & Staubo, E. F. 1993, Physical Review Letters, 70, 1355

Jaikumar, P., Prakash, M., & Schäfer, T. 2002, Phys. Rev. D, 66, 063003

Jaikumar, P. & Prakash, S. 2001, Physics Letters B, 516, 345

Kaaret, P., Prieskorn, Z., Zand, J. J. M. i., et al. 2007, ApJ, 657, L97

Kaminker, A. D., Haensel, P., & Yakovlev, D. G. 2001, A&A, 373, L17

Landau, L. D. & Lifshitz, E. M. 1980, Statistical physics. Pt.1, Pt.2, 3rd edn. (Oxford: Pergamon Press)

Lattimer, J. M. & Prakash, M. 2007, Phys. Rep., 442, 109

Lattimer, J. M., Prakash, M., Pethick, C. J., & Haensel, P. 1991, Physical Review Letters, 66, 2701

Leinson, L. B. & Pérez, A. 2006, Physics Letters B, 638, 114

Lombardo, U. & Schulze, H.-J. 2001, LNP, 578, 30

Miao, K. & Xiao-Ping, Z. 2007, MNRAS, 375, 1503

Miao, K., Xiao-Ping, Z., & Na-Na, P. 2007, [ArXiv:astro-ph/0708.0900]

Miralles, J. A. & van Riper, K. A. 1996, ApJS, 105, 407

Miralles, J. A., van Riper, K. A., & Lattimer, J. M. 1993, ApJ, 407, 687

Mühlschlegel, B. 1959, Zeitschrift für Physik, 155, 313

Niebergal, B., Ouyed, R., & Leahy, D. 2007, A&A, 476, L5

Özel, F. 2006, Nature, 441, 1115

Page, D., Geppert, U., & Weber, F. 2006, Nuclear Physics A, 777, 497

Page, D., Lattimer, J. M., Prakash, M., & Steiner, A. W. 2004, ApJS, 155, 623

Page, D. & Reddy, S. 2006, Annual Review of Nuclear and Particle Science, 56, 327

Pons, J. A., Link, B., Miralles, J. A., & Geppert, U. 2007, Physical Review Letters, 98, 071101

Potekhin, A. Y., Chabrier, G., & Yakovlev, D. G. 1997, A&A, 323, 415

Potekhin, A. Y. & Yakovlev, D. G. 2001, A&A, 374, 213

Reisenegger, A. 1995, ApJ, 442, 749

Schaab, C., Sedrakian, A., Weber, F., & Weigel, M. K. 1999, A&A, 346, 465

Schaab, C., Weber, F., Weigel, M. K., & Glendenning, N. K. 1996, Nuclear Physics A, 605, 531

Schaab, C. & Weigel, M. K. 1998, A&A, 336, L13

Schaffner-Bielich, J. 2007, [ArXiv:astro-ph/0703113]

Schmitt, A., Wang, Q., & Rischke, D. H. 2002, Phys. Rev. D, 66, 114010

Schulze, H.-J., Polls, A., Ramos, A., & Vidaña, I. 2006, Phys. Rev. C, 73, 058801

Steiner, A. W. & Reddy, S. 2009, Phys. Rev. C, 79, 015802

Steiner, A. W., Reddy, S., & Prakash, M. 2002, Phys. Rev. D, 66, 094007

Thorne, K. S. 1966, in Proc. Int School of Physics Enrico Fermi XXXV, ed. L. Gratton, (Academic: New York), 166

Van Riper, K. A. 1991, ApJS, 75, 449

Voskresensky, D. N., Yasuhira, M., & Tatsumi, T. 2003, Nuclear Physics A, 723, 291

Weber, F. 1999, Pulsars as astrophysical laboratories for nuclear and particle physics (IOP Publishing)

Weber, F. 2005, Progress in Particle and Nuclear Physics, 54, 193

Weber, F. & Glendenning, N. K. 1992, ApJ, 390, 541

Weber, F., Glendenning, N. K., & Weigel, M. K. 1991, ApJ, 373, 579

Xiaoping, Z., Li, Z., Xia, Z., & Miao, K. 2008, ArXiv e-prints, 0808.1587

Yakovlev, D. G., Kaminker, A. D., Gnedin, O. Y., & Haensel, P. 2001, Phys. Rep., 354, 1

Yakovlev, D. G., Levenfish, K. P., & Shibanov, Y. A. 1999, Soviet Physics Uspekhi, 42, 737

Yakovlev, D. G. & Pethick, C. J. 2004, ARA&A, 42, 169

Zdunik, J. L., Bejger, M., Haensel, P., & Gourgoulhon, E. 2006, A&A, 450, 747

This 2-column preprint was prepared with the AAS LaTeX macros v5.2.